Micro-architectural Features of the In Vivo Human Optic Chiasm

J. E. Sarlls[1], and C. Pierpaoli[1]

[1]NICHD, National Institutes of Health, Bethesda, MD, United States

Introduction

In this work, the micro-architecture of the optic nerves/chiasm/tracts were studied, in vivo, with diffusion tensor imaging (DTI) at sub-millimeter resolution. The optic chiasm is an interesting structure to study with DTI as it has intricate white matter architecture and could provide clinicaly relevant information in a number of conditions, such as optic pathway gliomas, pituitary tumors, and multiple sclerosis. However, the optic nerves/chiasm are a challenge to study with DTI utilizing a typical single-shot EPI sequence for two main reasons. First, the structures are located near sinus cavities and blood vesels, which are problematic for single-shot EPI as it is sensitive to susceptibility effects. Second, single-shot EPI is inherently limited in image resolution and the structures of interest are small in size. We have developed and implemented a radial fast spin-echo (FSE) sequence for high-resolution DTI in areas of susceptibility differences that allows sub-millimeter isotropic voxels to be acquired of in vivo brain [1]. We employed the radial-FSE sequence to acquire inter- and intra-subject DTI data of the optic chiasm wtih 10x smaller voxel volume than typically obtained with single-shot EPI.

Methods

Data were collected on a 3T GE Excite scanner with gradients capable of 40 mT/m and an 8-channel phased-array coil. T1-FLAIR images were acquired in an oblique plane at the angle of the optic chiasm with 0.9mm isotropic resolution and 0mm gap. The location of the T1-FLAIR slice that contained the optic nerves/chiasm/tracts was copied for the DTI acquisition, which consists of a single non-diffusion-weighted image along with b-value≈1000 s/mm^2 images in six non-collinear diffusion directions. Data of three healthy male volunteers were acquired at 0.9mm isotropic resolution (0.729mm^3 voxel volume) with the following scan parameters: TE =74ms, ETL = 4, and 512 radial lines collected with peripheral cardiac gating over 3 RxR intervals with minimum delay. To test the effects of slice thickness, DTI data collection was repeated on one volunteer with a 3mm slice. In addition, one volunteer underwent the data collection in three separate scan sessions, yielding data from three different superior locations of the optic chiasm. To reduce subject motion, a disposable bite bar was constructed, implemented, and secured to the coil.

Results

With the ability to collect DTI data at sub-millimeter resolution, partial volume effects are dramatically reduced allowing quantitative measures of the optic chiasm without CSF contamination. A representative directionally encoded color (DEC) map [2] calculated from one DTI data set is shown in **A**. The general DTI features of the optic chiasm region include a central area with strong anisotropy in the right/left direction (red) corresponding to the medial decussation of the nasal hemiretinae fibers, strong anisotropy in the anterior/posterior direction (green) corresponding to the non-crossing temporal hemiretinae fibers, and a newly revealed perimeter of low anisotropy surrounding the medial decussation. This perimeter is localized to areas consistent with sharp fiber curvature and/or complex crossings, which are known to reduce anisotropy measures. Further architectural information was obtained by calculating measures of the diffusion ellipsoid's shape, being linear and planar anisotropy [3]. In **B** the Westin-linear anisotropy is shown colored by the direction of the primary eigenvector and, expectedly, has similar appearance as the DEC map. In **C**, the Westin-planar anisotropy, representing the plane of fiber crossing, is shown colored by the direction of the third eigenvector (perpendicular to the plane of crossing). We observe a significant planar anisotropy component in the central chiasm. Using this additional information we detect the novel MR finding that, in the medial decussation, fibers are actually crossing with trajectories that contain a dorsal/ventral component rather than in a strictly right/left oriented line. Recent histological studies of human optic chiasm agree well with our observations [4]. The general features, linear and planar components of anisotropy in the central chiasm are consistent between subjects. In addition, we found that for data sets to exhibit the observed features of anisotropy it is necessary to acquire high-resolution data not only in-plane, but in the slice direction as well to avoid partial volume effects with CSF and between fiber populations.

Conclusions

Using the modified radial-FSE sequence, the optic nerve/chiasm/tracts can be studied in vivo with DTI. By acquiring sub-millimeter isotropic voxels, further architectural information can be gleened. We observe that there are micro-architectural differences not only in the medial and latteral regions of the optic chiasm, but also dorsal/ventral location which speaks to the evolving retinotopic organization from the optic nerve to the geniculate body. By acquiring DTI data at submillimeter resolution, tissue features, like planes of crossing fibers, can be well localized. This is in contrast to utilizing HARDI types of diffusion acquisitions to reveal multiple populations of crossing fibers within a large voxel; the proper fiber populations may be identified, but their location within the imaged voxel is unknown.

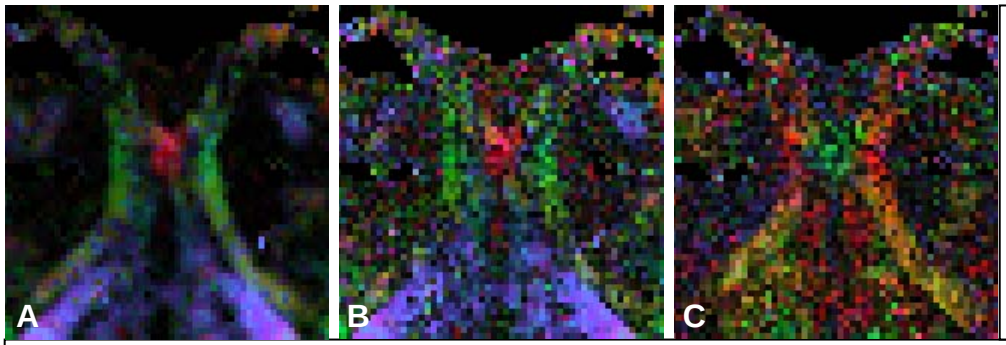

Images of DTI data acquired at 0.9mm isotropic voxels, 0.729mm^3, cropped to the optic nerves/chiasm/tracts region. DEC map is shown in **A**. Corresponding Westin-linear anisotropy map colored by the direction of the primary eigenvector is shown in **B**. The corresponding Westin-planar anisotropy map colored by the third eigenvector, the direction perpendicular to the plane, is shown in **C.** The R/L direction is red, A/P direction is green, and S/I direction is blue. Note, fibers in the medial decusation have a linear component in the R/L direction, and a planar component perpendicular to A/P.

References: [1] Sarlls *et. al.,* MRM, 60: 270-276, 2008. [2] Pajevic *et. al.,* MRM, 42: 526-540, 1999. [3] Westin *et. al.,* MIA, 6: 93-108, 2002. [4] Neveu *et. al.,* EJN, 23: 3034-3042, 2006.